NASA TECHNICAL MEMORANDUM

NASA TM X-67984

NASA TM X-67984

EXPLORATORY SCREENING TESTS OF SEVERAL ALLOYS AND COATINGS FOR AUTOMOBILE THERMAL REACTORS

by Robert E. Oldrieve
Lewis Research Center
Cleveland, Ohio
December, 1971

This information is being published in preliminary form in order to expedite its early release.

ABSTRACT

A total of 23 materials (that included uncoated ferritic and austenitic iron-base alloys, uncoated nickel and cobalt-base superalloys, and several different coatings on AISI 304 stainless steel) were screened as test coupons on a rack in an automobile thermal reactor. Test exposures were generally 51 hours including 142 thermal cycles of 10 minutes at 1010°±30° C (1850°±50° F) test coupon temperature and 7-minutes cool-down to about 510° C (950° F). Materials that exhibited corrosion resistance better than that of Hastelloy X include: a ferritic iron alloy with 6 weight percent aluminum; three nickel-base superalloys; two diffused-aluminum coatings on AISI 304; and a Ni-Cr slurry-sprayed coating on AISI 304. Preliminary comparison is made of the performance of the directly impinged coupons and a reactor core of the same material.

E-6717

TABLE OF CONTENTS

EXPLORATORY SCREENING TESTS OF SEVERAL ALLOYS AND COATINGS FOR AUTOMOBILE THERMAL REACTORS

by Robert E. Oldrieve

Lewis Research Center

SUMMARY

Preliminary evaluation was made of twenty-three (23) candidate automobile thermal reactor materials (including thirteen uncoated alloys and nine coatings on AISI 304 stainless steel) in coupon screening tests conducted in a reactor on an engine-dynamometer test stand. Test cycles consisted of 10 minutes at 1010°±30° C (1850°±50° F) followed by cool-down to a coupon temperature of about 510° C (950° F) for a total elapsed time of 17 minutes per cycle.

The severity of the screening test coupons exposure is such that test coupons are attacked at about 3 times faster than the test core and about 3 to 4 times that of baffle plates in a reactor exposed using a modified AMA city driving schedule. In the generally applied 143-cycle exposure, Hastelloy X coupons lost about 0.2 mm (8 mils) or 47 mg/cm^2. Uncoated materials were considered to have failed when the weight-loss exceeded that of Hastelloy X. Coated materials were kept in test until the weight loss exceeded the as-deposited coating weight-gain (usually followed by the accelerated rate of oxidation of the uncoated AISI 304 material).

Based on these criteria the best materials of those tested are as follows:

Alloys (uncoated)

Ferritic iron alloy: Fe-Cr-Al type (Hoskins 875)
Nickel base alloys: Inconel 601, René 41, Inconel W

Coatings (on AISI 304 substrate)

Slurry-applied nickel-chromium coatings: NC-630
Diffused-aluminide coatings: Al and Ni-Cr/Al

E-6717

INTRODUCTION

One of the more effective pollution control devices which has been developed to clean-up automobile engine exhaust is a thermal reactor (refs. 1, 2, and 3). In a thermal reactor, unburned hydrocarbons and carbon monoxide are oxidized by reaction with injected air to produce primarily water and carbon dioxide. From the oxidation process, the core of a thermal reactor reaches temperatures from about 870° C (1600° F) to

1040° C (1900° F) under normal driving conditions. This high temperature oxidizing environment, in combination with high velocities and corrosive constituents in the exhaust gas, presents a severe environment for potential reactor materials. Whereas nickel-base alloys might meet most of the reactor requirements, their relatively high cost and the limited supply of nickel preclude a widespread use of these materials.

The purpose of this report is to summarize the results of an exploratory screening test program of candidate materials for use in an automobile thermal reactor. A relatively broad compositional range of sheet materials with demonstrated moderate to high temperature capability in an oxidizing environment were evaluated. They included thirteen uncoated alloys (including ferritic-iron-base alloys, austenitic stainless steels, and nickel and cobalt-base superalloys) and nine different oxidation-resistant coatings on AISI 304 stainless steel. Test coupons of each test material were mounted in a thermal reactor and exposed to exhaust gas from an automobile engine operated in a cyclic mode for exposures which range from 48 cycles (16 hr) to 308 cycles (110 hr). Each test cycle consisted of approximately 10 minutes at a coupon test temperature of 1010°±30° C (1850°±50° F) followed by seven minutes with the engine idling to reach 510° C (950° F) before return to peak temperature. The test materials were evaluated on the basis of weight and thickness change with supplemental metallography and measurement of unaffected substrate thickness.

This program was conducted in cooperation with the Office of Air Programs of the Environmental Protection Agency.

MATERIALS AND PROCEDURE

Materials Evaluated

Alloys. - Selection of alloys was made to include a wide composition range of sheet materials reported to possess high temperature oxidation resistance. Two ferritic iron-base alloys, five austenitic iron-base alloys, six nickel-base superalloys, and one cobalt-base superalloy were included with the nominal compositions listed in table I. Hastelloy X, RA 333, and Hoskins 875 were selected because of their good cyclic oxidation resistance exhibited at 760° to 1200° C (1400° to 2200° F) in a high temperature sheet alloy program (ref. 4). HS-188, E-Brite, and Inconel 601 were submitted by their manufacturers as alternate potential candidates. And René 41, René 62, and Inconel W were included as representative highly alloyed sheet materials with superior high temperature strength and generally good oxidation resistance. No special surface treatment or preparation was used. All uncoated materials were evaluated in standard mill-annealed condition.

Test coupon size was generally 1.9 cm (0.75 in.) by 5 cm (2 in.) and thickness ranged from 0.7 mm (0.027 in.) to 1.7 mm (0.067 in.).

Coatings. - Eight commercially produced coatings and one NASA-Lewis developed coating (ref. 5) were applied to test coupons of AISI 304 stainless steel. The coating identifying key used throughout this report and pertinent information supplied for each of the coatings are listed in table II. Five compositions of slurry-applied nickel-chromium coatings were submitted by a coating vendor. The glass coating systems were submitted in response to a request made of members of the Porcelain Enamel Institute and were furnished as-sprayed and sintered by the coating vendor. The nominally unalloyed aluminide coating was applied using pack-cementation techniques. The NASA coating is a flame-sprayed nickel-chromium alloy, which was then pack-aluminized. The as-coated thicknesses of all coatings listed in table II were determined metallographically and the coating deposition amounts tabulated in table II are estimated based on known or calculated coating density.

Test Procedure

The coupons of materials to be tested were installed on a rack in a test specimen reactor mounted on an automobile engine in the place of the cast-iron exhaust manifold (fig. 1). In general, two test specimens were placed at each exhaust impingement location (baffle location, fig. 2). A limited comparison of results obtained for specimens mounted in a nonimpingement "gusset" location is made for uncoated AISI 304, AISI 310, and AISI 651 alloys. The automobile engine was mounted on a test stand and was coupled at first by a universal coupling and later by automatic transmission to a motor-generator dynamometer mounted on the same test bed (see fig. 3). The weight change of uncoated AISI 304 stainless steel test coupons was used as a control verification to indicate the degree of test repeatability and test coupon exposure uniformity at various locations throughout the test series.

Test engine. - The test engine was selected because of its existing air injection system and is a 472 (cubic inch displacement), 1969 model year, 90° V-8 Cadillac engine which is rated by the manufacturer at 375 horsepower at 4400 rpm. The standard injection air pump output to each bank of four cylinders was used as furnished and was found to provide the desired 1040° C (1900° F) test coupon metal temperature, using the test reactors, without change in carburetor jets, engine timing, or spark advance normally used by the manufacturer for the 1969 air injection system. The air to each cylinder bank was diverted, however, to provide measurement and equilibration through calibrated flow meters (air rotometers).

Test reactors. - Drawings of the test specimen reactor are shown in figures 1 and 2. The assembly consists of: an outer shell and end flanges of AISI 304 stainless steel; and a reactor core, interior necks, end plates, and double-wall all-metal insulation liner of Hastelloy X. The coupons in the test specimen reactors were at first wired, then riveted, and finally bolted in place during the course of eight test-exposure series (rivets were best for long exposure periods, but they

presented problems in specimen removal). Thermocouples were mounted on test specimens, on the test specimen rack, and in the reactor exhaust pipe to determine the reactor metal temperature distribution and operating conditions.

A second type of reactor, without test specimens and with an aluminized Incoloy-800 core (Type VI, ref. 6), was subjected to the same test cycle used for the test coupon materials evaluation. This additional test was performed to afford comparison of the durability of baffle coupon and test reactor core materials with data obtained by others (ref. 2) in chassis-dynamometer endurance evaluation for exposures for up to 160 000 km (100 000 miles).

Test cycle. - The test cycle provided peak test coupon temperatures of about 1040° C (1900° F) for 10 minutes each cycle with a subsequent seven minute cool-down to temperatures encountered at idle conditions and return to peak temperature. Test coupon temperatures were measured by thermocouples inserted in sheaths tack-welded to the lower specimen surface (opposite the gas-impingement surface) of uncoated specimens. The engine-dynamometer conditions found to provide the peak specimen temperature were 3000 engine rpm, 15 cm (6 in.) Hg manifold vacuum and approximately 150 horsepower absorbed by the dynamometer. The variation of temperature from specimen to specimen is shown in figure 2 and is typically 1010°±30° C (1850°±50° F). The temperature spread is believed to be quite satisfactory for this program. It is noted that the reactor core wall temperatures (also shown in fig. 2) indicate general temperature uniformity throughout the core region. The specimen temperatures at idle conditions and with continued injection of reactor air were found to drop to a nominal 565° C (1050° F) at 1000 engine rpm and 50 cm (20 in.) Hg manifold vacuum after five minutes and subsequently to about 510° C (950° F) as a minimum. The total cycle was at first manually and later automatically controlled. For automatic operation at the later stages of the program, an automatic transmission and engine rpm control circuit were used. To enable use of an automatic transmission, it was convenient to preset the peak dynamometer load such that under engine idle operation the minimum cycle temperature was generally increased to 620° C (1150° F) after 5-1/2 minutes in the 1000 rpm mode (still with seven min. time between the 10 min. peak temperature operation). For the automatic operation the engine rpm was controlled to ±25 rpm using a magnetic and an electro-pneumatic circuit to provide throttle control.

Evaluation Methods

Measurements. - Test specimen coupon weights are reported as-brushed (to remove loose oxide) and as-dimensionally-measured for thickness prior to testing, at periodic intervals, and after test exposure. Test data are reported as weight-change in mg/cm^2 of test coupon surface. Test specimens of materials which had not failed (based upon weight loss criteria) were metallographically sectioned to obtain a measure of the thickness of unaffected substrate.

Failure criteria. - Failure criteria used as the basis for the discussion of results were somewhat arbitrarily selected as follows:

1. Uncoated alloys were considered to have failed when the weight-loss was greater than that of Hastelloy X after 142 cycles (i.e., weight-losses greater than 47 mg/cm^2). From prior work (ref. 2), it was known that Hastelloy X survived the equivalent of 96 000 km (60 000 miles) of the Modified AMA City Driving Schedule before onset of baffle plate failure.

2. Coated test specimens were considered to have failed either when the slope of the weight loss curve approached that of the uncoated alloy or when approximately 20 mg/cm^2 was lost (equal to or greater than the as-deposited weight for all the coatings except NC-630, NC-700, and Ni-Cr/Al which were in the range of 30 to 46 mg/cm^2).

For both coated and uncoated materials, it is recognized that weight change alone is a poor measure of oxidation resistance. At the extreme, a metal can be completely converted to oxide and during the oxidation process can continue to gain weight (if the oxide does not spall) until the specimen fails from lack of strength. However, a review of the weight change results revealed that the specimens generally lost weight throughout the screening tests so that screening using the above criteria can be applied.

Test coupons were tested in duplicate only where confirmation of marginally-rated material was sought, where longer term data was desired, or where specimens were candidates for use as control material (AISI 304, AISI 651, and AISI 310 alloys).

RESULTS AND DISCUSSION

Plots of weight change (in mg/cm^2) against the number of screening test cycles of exposure are presented in figures 4 through 7 and are discussed by category of materials and coating systems below.

Uncoated Alloy Test Coupons

Ferritic iron-base alloys. - In a test of limited duration of two ferritic alloys, both appear to have considerable oxidation resistance based on weight change alone (fig. 4). The E-Brite alloy gained only 4.8 mg/cm^2 in 48 test cycles and the Hoskins 875 alloy lost less than 1 mg/cm^2 in 80 test cycles. The E-Brite alloy, however, grew 178 μm (7 mils) in thickness thereby indicating considerable conversion of the alloy to oxide and unsatisfactory performance in comparison with the less than 15 μm (0.6 mils) growth of the Hoskins 875 test coupon after the same 48 cycle exposure. A photograph of the alloy test coupons after 48 cycles is shown in figure 8. The test was terminated after 80 cycles because the E-Brite attachment failed between 48 and 80 test cycles. Be-

cause the two alloy compositions are similar (table I) except for aluminum content, it appears that aluminum additions can impart considerable oxidation resistance to a ferritic 23 to 26 weight percent chromium alloy for this application. Based on these results, Fe-Cr-Al alloys of the Hoskins 875 type warrant further evaluation for reactor use.

Austenitic iron-base alloys. - The austenitic iron-base alloys all lost appreciably more weight than either of the ferritic iron-base alloys evaluated, as is shown in figure 4. Based on the failure criteria used here, all of these austenitic alloys are considered to have failed this test. As previously mentioned, the AISI 304 alloy was used as a control for most of the screening program. This selection was made because the AISI 304 test coupons were found to lose weight at a reasonably consistent rate in this test and were found to realize the consistent-rate loss no matter where they were placed within the test reactor. In figure 4 the rack-exposed ("baffle") test coupon data are plotted as open symbols. The data for coupons exposed below the rack ("gusset" location) are plotted as closed symbols. For AISI 304 it was noted that the data fall in a relatively narrow band for test coupons exposed at baffle and gusset locations, for several rack positions, and for exposures on either side of the engine. The AISI 304 stainless steel lost about 100 mg/cm^2 and 180 μm (0.007 in.) in thickness in 97 test cycles. The data spreads for AISI 651 and AISI 310 coupons were greater and resulted from apparent differences in adherence of the protective oxides combined with mechanical causes of oxide spalling (vibration or specimen deformation). Gusset samples, for example, were constrained only at one end and were free to warp and cause spallation. Generally, it was observed that: the exposed specimens of AISI 304 had little or no adherent oxide upon cool-down; the AISI 651 specimens were completely covered with an adherent oxide layer; and the AISI 310 specimens were only partially covered with the remainder of an oxide layer (which completely spalled upon cool-down for a 48-cycle exposed specimen with a weight loss of 155 mg/cm^2).

From figure 4, it is seen that A-286 is the best of the austenitic iron-base alloys evaluated. This somewhat better performance may be due to its titanium and aluminum content. But A-286 also failed the test based on the failure criteria and was found to have gained 152 μm (0.006 in.) in thickness after the full-term 142-cycle test exposure.

Superalloys. - The weight change data shown in figure 5 rank seven superalloys in terms of increasing weight-loss after 142 cycles in the order of Inconel W and René 41 as best with less than 2 mg/cm^2 weight change, then Inconel 601 with an acceptable 7 mg/cm^2 loss, followed by RA 333, Hastelloy X, and HS-188, all with greater than 40 mg/cm^2 loss. Comparison of these alloys by major constituents is tabulated in table I. Based on weight change and composition alone, it may be noted that the three best superalloys contain greater than 60 weight-percent nickel. These three alloys contain aluminum (greater than 0.5 percent), no tungsten, and the two best (based on weight-change) contain titanium (greater than 2.5 percent). It appears likely that these compositional differences from the intermediate-nickel-content Hastelloy X and RA 333 alloys

promote oxidation resistance for the automobile reactor application. (It is noted that René 41 has molybdenum content equal to that of Hastelloy X and that both Inconel W and René 41 have appreciably less chromium than the intermediate-nickel-content alloys.) Limited data for René 62 alloy are an exception unless the high chromium content has unexpected significance in causing deterioration of superalloys in an exhaust gas environment. The René 62 alloy (with 23 weight percent chromium and a total of about 12 weight percent Mo + Cb) lost an unacceptable 15 mg/cm^2 in only 40 test cycles. As discussed in the formulation of failure criteria based on weight loss it was generally noted for the superalloys that those that lost appreciable weight were found to have only thin layers of oxide remaining after test exposure. The three best superalloys (based on weight-loss alone) had relatively thick adherent oxides such that René 41, Inconel W, and Inconel 601 gained 86.4 μm (0.0034 in.), 46 μm (0.0018 in.), and 50 μm (0.002 in.) in coupon thickness, respectively. Evidence of oxide spall is apparent for the intermediate nickel content alloys but was not found for those with thicker adherent oxides.

The conclusion made from the superalloy test data was to continue testing of Inconel 601 beyond 142 cycles because of its lower cost in comparison with the others and its nearly equivalent oxidation resistance. Photomicrographs of Inconel 601 as-received and after 267 test cycles (fig. 9) reveal that a relatively thick 100 μm (0.004 in.) oxide layer remains after a nearly 30 mg/cm^2 weight-loss. Thus, a considerable fraction of the coupon thickness has been consumed in addition to loss of section thickness as the result of 75 μm (0.003 in.) intergranular oxidation. In addition, substrate grain growth and possible internal oxidation may be observed. Owing to the low cost of Inconel 601 superalloy and considering that a total of 0.36 mm (14 mil) loss of unaffected substrate thickness may be fully acceptable for an automobile thermal reactor, it is concluded that Inconel 601 warrants still further evaluation for this application.

In addition to the nickel-based superalloys discussed above, evaluation was made of the cobalt-based superalloy HS 188. This alloy lost 112 mg/cm^2 and 57 μm (0.0023 in.) in thickness after 170 test cycles, thus tending to preclude its consideration for automobile thermal reactor application. This result was somewhat surprising because this alloy was developed for high temperature oxidation resistance. Thus test coupons were metallographically examined to seek the cause of this relatively poor performance. Photomicrographs of the material as-received and after 170 test cycles are presented in figure 10. It is noted that a semiporous oxide scale formed on the surface (probably a cobalt-chromium mixed oxide based on green and blue phases in polarized light). Intergranular oxidation occurred directly (one grain) ahead of the oxidation front (black oxide fingers in polarized light). On the underside of the test coupon, the oxide is about four times thicker than shown on the impingement surface of figure 10(b). No evidence of internal oxidation, change in dispersed structure, or grain growth is seen. Thus it is concluded that the poorer performance of this alloy is probably due to the lack of protection of the oxide scale under these test conditions.

Coated AISI 304 Test Coupons

Ni-Cr slurry coatings. - The weight-change data for five Ni-Cr coating compositions applied to AISI 304 alloy test coupons are given in figure 6. The data show that NC-630 coating has the least weight loss. However, visual examination of the impingement surface of this specimen reveals a mottled appearance, and metallography (fig. 11) indicated that local penetration of the NC-630 coating has occurred at the mottled (corrosion pit) areas (fig. 12). Very little spall and no coating unbonded areas were observed for this system.

Coating NC-610, which has the second ranking based on weight loss, has only a loosely-adherent oxide as can be seen by its flaky appearance in figure 12. In the same figure the NC-9 coating is seen to retain its metallic luster over perhaps one-third of the coupon, but it has a net weight loss of nearly twice the amount lost by the NC-610 specimen.

Duplicate specimens of NC-630 and NC-610 coated coupons were tested (plotted as dashed lines in fig. 6) to verify these limited results. One of the NC-610 specimens spalled more excessively than the other, whereas the NC-630 specimens more closely duplicated each other to substantiate the apparent superiority of the NC-630 coating system in these tests on the AISI 304 alloy substrate.

The other two systems, NC-6 and NC-700, spalled excessively after 67 and 108 test cycles, respectively, such that the NC-700/AISI 304 system lost weight at about the same rate as the uncoated AISI 304 substrate.

From these data, I conclude that none of the Ni-Cr slurry-applied coating systems tested are completely satisfactory for the protection of AISI 304 using this screening test exposure. Because the NC-630 coating survived the 142 cycle exposure with a reservoir of coating away from the corrosion pit areas and because this coating is potentially less costly to apply than others, further study may be warranted but preferably on a stronger substrate such as may be required for a thermal reactor. The NC-630 coating was adherent, appears to be metallurgically bonded, and is of a basic composition (Ni-Cr) which would be expected to be oxidation resistant. A substrate which does not deform as readily may eliminate the possible intergranular cracking and oxidation within the coating layer seen at the right-hand side of figure 11.

Glass coatings. - The weight-change data for two glass-based coating compositions are included in figure 7. Both of these coatings exhibited little weight change for the first 50 cycles, but only the coating designated Glass-2 has survived the screening test exposure. The Glass-2 coating differs from Glass-1 only by the inclusion of 90 weight-percent Ni-Cr particles which may aid in preventing coating spall found to be the mode of failure of Glass-1 in duplicate tests. The Glass-2 coating with included metal particles is seen to allow substrate oxidation, nonetheless (fig. 12). Because of the high metallic content of the glass coating which survived and the probable lack of any advantage over that of slurry

or spray-applied all-metal coating systems, neither of these glass-based coatings appear to warrant further study.

Aluminide coatings. - Two different types of diffused aluminum (aluminide) coatings were tested and evaluated. One of these (designated Al) was diffused (by pack cementation) directly into the surface of the AISI 304 substrate while the other (designated Ni-Cr/Al) was applied after the substrate was first flame-sprayed with 80 nickel-20 chromium (by weight percent) alloy powder (see table II). The results of the reactor tests on these specimens are shown in figure 7 for comparison with the best of the other candidate coating systems.

Both of the aluminide coatings performed well for the nominal 142 cycle exposure (i.e., less than 5 mg/cm^2 weight loss for the Al coating and less than about 10 mg/cm^2 weight gain for Ni-Cr/Al). The Ni-Cr/Al coupon which was continued in testing began losing weight thereafter until, at 308 cycles the coupon lost about 1.7 mg/cm^2.

Photomicrographs of the Al and Ni-Cr/Al coated specimens in the as-coated condition are nearly identical in appearance and in depth of aluminum penetration as typically shown for an Al coated specimen in figure 13(a). The major coating phase in the outer layer, however, is Cr_3Al_2 for the typical Al system and Ni_2Al_3 for the Ni-Cr/Al system (ref. 5). After 142 and 132 cycles, respectively, both the Al and Ni-Cr/Al coatings show nearly identical 0.13 mm (0.005 in.) penetration of the substrate by aluminum (figs. 13(b) and 14(a)). The Al system (fig. 13(b)), however, is seen to be partially penetrated at local sites by oxide and appears to be oxidized beneath the outer coating layer (separation seen in fig. 13(b) may have resulted from metallographic preparation). The Ni-Cr/Al system appears to allow a more general consumption of the outer coating, greater oxide retention, and, possibly, less void and internal oxidation. After 308 cycles, the aluminided substrate (MAl) layer of the Ni-Cr/Al coating, was depleted to a thickness of less than 0.05 mm (0.002 in.) indicating that no more than twice this life is likely to be obtained. Also at 308 cycles it can be seen that the Ni-Cr/Al coated test coupon has grown in dimensions and the test coupon has cracked (fig. 15). The cracking was caused by constraint of the specimen and buckling of the test coupon. In figure 15(b) a local site denoted "star failure" is the only indication found of a defect solely attributable to the Ni-Cr/Al coating system.

Based upon the test criteria and sparsely located sites of failure, further study of aluminided coatings for stainless steels is warranted. The Ni-Cr/Al coating provided the best oxidation protection and the Al coating the second-best of the nine coating compositions evaluated in this program.

Comparison of Results for Test Coupons and Reactor Core Components

An estimate of the severity of these screening test results on

directly-impinged test coupons as compared with the performance of full-scale reactor core components made of the same material can be made for Hastelloy X. Hastelloy X was evaluated as both test coupons and as the reactor core in this program.

The metal loss rates of the Hastelloy X coupon and the test reactor core at the areas of greatest apparent erosion were determined metallographically by measuring the remaining base metal below the oxide layer at the completion of the test exposures (table III). Also included in table III is the metal loss-rate measured at impingement areas (opposite exhaust ports) of a full-size emissions-type reactor with aluminized Incoloy-800 alloy core. Both the Hastelloy X core and the aluminized Incoloy-800 alloy core were intact after the tabulated exposure times; however, the latter core was denuded of coating at the impingement areas.

From the tabulated results of the screening test exposure, it can be seen that the Hastelloy X test coupon lost weight nearly three times faster than the Hastelloy X core. For screening purposes the rack-mounted ("baffle") test coupon location appears to provide the most accelerated corrosion of a candidate reactor core material. A material which survives in the test coupon location may survive up to three times longer as a thermal reactor core.

A further estimate of the severity of the screening test cycle may be made by projecting to failure of the test coupons and comparing expected life with the known life of baffle components which have failed in simulated (chassis-dynamometer) automobile service (ref. 2). In reference 2, data are presented which show that 2.8 mm (0.11 in.) thick Hastelloy X baffle plates were penetrated after 1900 to 3200 hours (96 000 to 160 000 km or 60 000 to 100 000 miles) exposure using the relatively "easy" Modified AMA City Driving Cycle (but with 1010° C (1850° F) peak reactor temperature for two brief periods in each 40 miles). Based on the metal loss rate indicated in table III for Hastelloy X coupons using the screening test cycle of this program, complete loss of 2.8 mm thick coupons could be expected to occur in about 700 hours rather than the 1900 to 3200 hours of reference 2. Thus, it might be tentatively concluded that the screening test conditions used in this program are about 3 to 4 times more severe than Modified AMA City Driving Cycle service. This is further substantiated by comparing the results from aluminized Incoloy-800 full reactor cores (1.5-mm, 0.060-in., thick) which were penetrated in 80 000 kilometers (50 000 miles) Modified-AMA-Cycle chassis-dynamometer testing or about 1600 hours (ref. 2). From the loss rates listed in table III for an identical full-size reactor material exposed to the screening test cycle, this thickness of material can be projected to fail in about 400 hours. Again for reactor cores as well as for baffle plates, the screening test cycle appears to be about 3 to 4 times more severe than the Modified AMA City Driving cycle.

It is concluded, by making these comparisons, that the screening test exposure appears to be at least 3 times more severe than might be

expected in service and that the test duration for the cores and coupons (50 to 100 hr) is at least 10 to 20 percent of the desired life of the materials evaluated if they were used in thickness of 1.5 mm (0.060 in.).

CONCLUSIONS

Based on the results of the screening test of coupons of 23 materials exposed to the direct impingement of automobile exhaust products, the following materials warrant further evaluation for use in automobile thermal reactors:

Alloys (uncoated)

Ferritic iron alloy: Fe-Cr-Al type (Hoskins 875)
Nickel base alloys: Inconel 601, René 41, Inconel W

Coatings (on AISI 304 substrate)

Slurry-applied nickel-chromium coatings: NC-630
Diffused-aluminide coatings: Al and Ni-Cr/Al

CONCLUDING REMARKS

Representative materials of each of those types which survived this screening program are being evaluated as full-size reactor cores in a related program being conducted under NASA-contract at Teledyne-Continental Motors, Muskegon, Michigan. Initial results of this related program are reported for up to 200 hours of test exposure in reference 8. It is noted that other Fe-Cr-Al alloys are included in the full core program because of the relatively low cost and good performance of this type of alloy. Aluminide coatings selected include chromium-aluminum diffusion coatings but exclude, for the time being, the Ni-Cr/Al coating because of the costly application techniques required (i.e., plasma-spray Ni-Cr followed by pack-cementation Al).

REFERENCES

1. Brownson, D. A.; and Stebar, R. F.: Factors Influencing the Effectiveness of Air Injection in Reducing Exhaust Emissions. Paper 650526, SAE, May, 1965.

2. Cantwell, E. N.; Rosenlund, I. T.; Barth, W. J.; Kinnear, F. L.; and Ross, S. W.: A Progress Report on the Development of Exhaust Manifold Reactors. Paper 690139, SAE, Jan. 1969.

3. Oldrieve, Robert E.; and Saunders, Neal T.: Materials Problems in Automotive Exhaust Reactors for Pollution Control, Aerospace Structural Materials. NASA SP-227, 1970, pp. 317-330.

4. Cole, Fred W.; Padden, James B.; and Spencer, Andrew R.: Oxidation Resistant Materials for Transpiration Cooled Gas Turbine Blades. I. - Sheet Specimen Screening Tests. NASA CR-930, 1968.

5. Klechka, Ernest W.; and Grisaffe, Salvatore J.: Exploratory Studies on Modified Aluminide Coatings for Low Carbon and Stainless Steels. NASA TM X-2201, 1971.

6. Cantwell, E. N.; et al.: Recent Developments in Exhaust Manifold Reactor Systems. Presented to the Automobile Division, The Institution of Mechanical Engineers, London, England, May 1970. (Paper available from E. I. duPont de Nemours & Co., Inc., Wilmington, Dela.)

7. U. S. Department of Health, Education and Welfare, Part II: Control of Air Pollution from New Motor Vehicles and New Motor Vehicle Engines Federal Register, vol. 35, no. 219, Nov. 1970.

8. Oldrieve, R. E.: Evaluation of Some Candidate Materials for Automobile Thermal Reactors in Engine Dynamometer Screening Tests, NASA TM X-67970.

TABLE I
COMPOSITIONS OF SHEET ALLOYS EVALUATED

Alloy Designation	Nominal Compositions[1] (percent by weight)												
	Fe	Cr	Al	Ni	Co	Mo	W	Ti	Si	C	Mn	N	Other
Ferritic Iron-Base Alloys													
E-Brite[1]	72	26.2	0.01	0.09	—	0.98	—	—	0.24	-	0.02	0.01	—
Hoskins 875	71	23	6	-	-	-	—	—	—	-	-	-	-
Austenitic Iron-Base Alloys													
AISI 304	71	18.5	-	9.5	—	—	—	—	—	0.08	—	-	—
AISI 651(19-9DL)	70	18.5	-	9	-	1.4	1.4	0.25	0.55	0.32	1.15	—	0.4(Cb+Ta)
AISI 310	54	25	-	20	—	—	—	—	—	0.25	—	-	—
A-286	54	15	0.2	26	-	1.3	-	2.0	0.5	0.05	1.35	—	—
Incoloy-800[2]	46	20.5	0.4	32	—	-	-	0.4	-	0.04	—	—	—
Nickel-Base Superalloys													
Rene' 62[1]	23	14.5	1.2	71	—	8.89	-	2.34	0.09	-	—	—	3.1 Cb
Hastelloy X	18.5	22	—	52	1.5	9	0.6	—	0.5	0.1	0.5	-	—
RA 333[1]	17.8	25.2	—	45.11	-	3.01	3.06	-	1.20	0.05	1.65	—	—
Inconel 601	14.1	23	1.35	60.5	—	-	-	—	0.25	0.05	0.5	—	—
Inconel W	8	14.5	0.6	75	-	—	—	2.7	0.5	0.03	—	-	—
Rene' 41	5	18.5	1.5	60	11.5	9.5	—	3.2	0.5	0.09	0.1	-	-
Cobalt-Base Superalloys													
HS-188	1.5	22	-	22	36.4	-	15.5	-	0.4	-	2.0	-	0.8 La

(1) - Compositions listed are nominal except those noted (1) for which actual analyses are provided.

(2) Incoloy 800 is used as a coating substrate.

TABLE II

COATING SYSTEMS EVALUATED ON AISI 304 COUPONS

COATING KEY	COATING COMPOSITION (NOMINAL)	APPLICATION METHOD (1) & PARAMETERS	AMOUNT DEPOSITED mg/cm^2	THICKNESS μm	COATING VENDOR	DESIGNATION
NC-6	Ni-7Cr-6W-5Si-2Fe-3B	H_2, 30min, 1150°C	14.9	20.2	WALL COLMONOY	NICROCOAT 6
NC-610	Ni-14Cr-10TiB_2	VAC., 30 min, 1150°C	21.9	30.6	WALL COLMONOY	NICROCOAT 610
NC-9	Ni-19Cr-10Si-5(OTHER)	H_2, 30min, 1150°C	20.2	28.0	WALL COLMONOY	NICROCOAT 9
NC-630	Ni-17Cr-5Si-7Ti_5Si_3-7TiN	VAC., 30min, 1150°C	47	66.0	WALL COLMONOY	NICROCOAT 630
NC-700	Ni-13Cr-10TiB_2-5Al_2O_3	VAC., 30min, 1150°C	46	63.5	WALL COLMONOY	NICROCOAT 700
Glass-1	25SiO-17Cr_2O_3-63 Barium glass frit.	Air, 10min, 1040°C	18.6	89.0	CHICAGO VITREOUS	SL-14230
Glass-2	90 NICROCOAT 6 (see above) + 10 Barium glass frit.	Air, 10min, 1090°C	23.8	114.0	CHICAGO VITREOUS	SL-15864
Al	MAl (where M=AISI304)	pack cementation (parameters proprietary)	8.6	25.4	CABOT CORP.	WL-1
Ni-Cr/Al	Ni_2Al_3 + CrAl	Ni+Cr: flame-sprayed Al: pack(2), Argon, 16hrs, 871°C	15 Ni-Cr AND 17 Al = 32	158	NASA-Lewis	Ni-Cr/Al

(1) All sprayed, dried, and sintered at tabulated conditions, except as noted.

(2) Pack cementation: pack composition: 2%Al-96%Al_2O_3.

TABLE III

COMPARISON OF TEST COUPONS AND REACTOR CORES

Material (test piece)	Metal Loss Rate mm/hr. (mils/hr)	Hours in test*	Time to produce 1.54 mm. metal loss (Hours)
Hastelloy X (coupon)	0.0041 (0.163)	51	380
Hastelloy X (core)	0.0015 (0.0055)	110	1100
Al/Incoloy-800 (core)	0.0037 (0.145)	48	432

* Cycle consisted of 10 minute exposure at 1010°±30°C (1850°±50°F) followed by a 7 minute exposure with 510°C (950°F) minimum test coupon metal temperature.

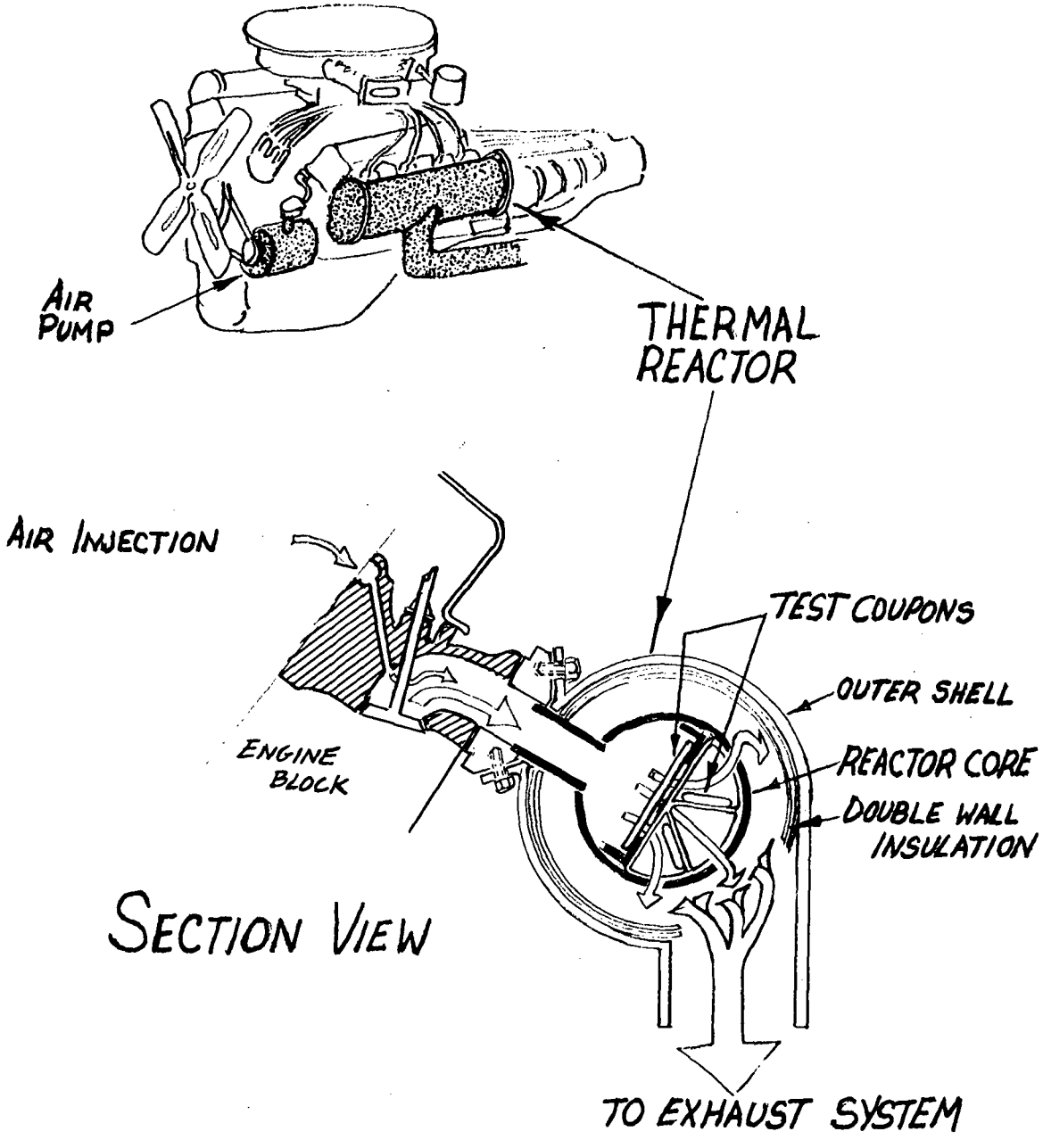

Figure 1. - Thermal reactor installation on engine.

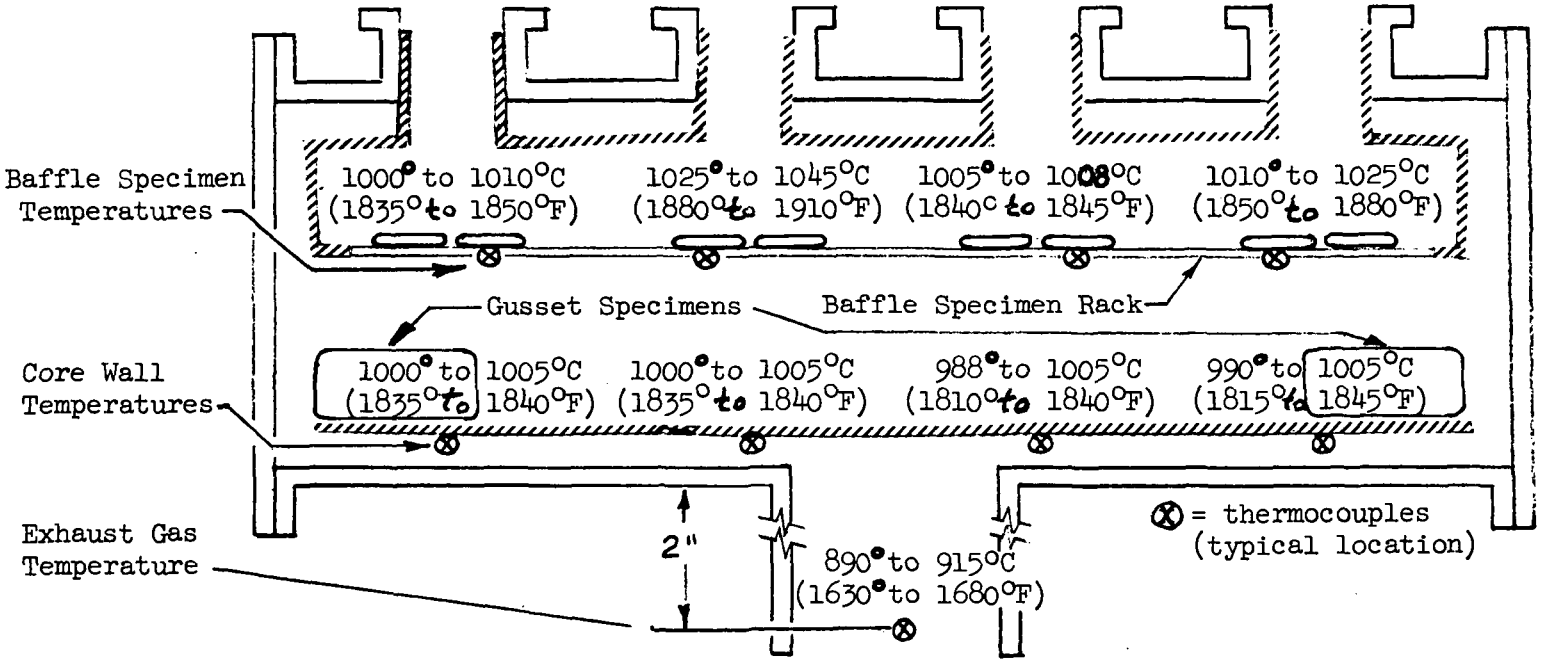

FIGURE 2 - Thermal reactor longitudinal section showing test specimen and reactor core-wall temperature distribution and range for a typical test series.

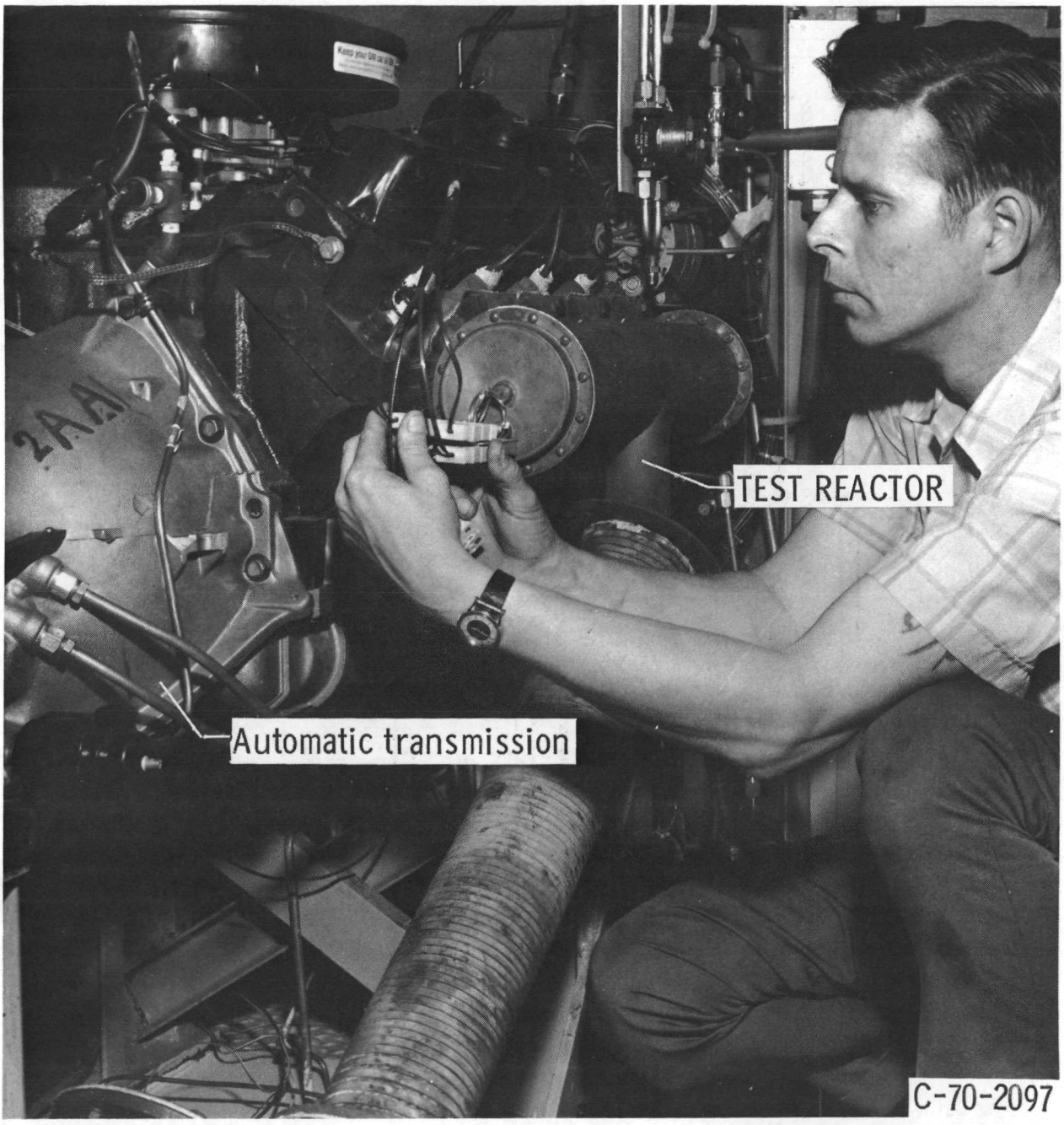

Figure 3. - Engine test stand showing reactor installation.

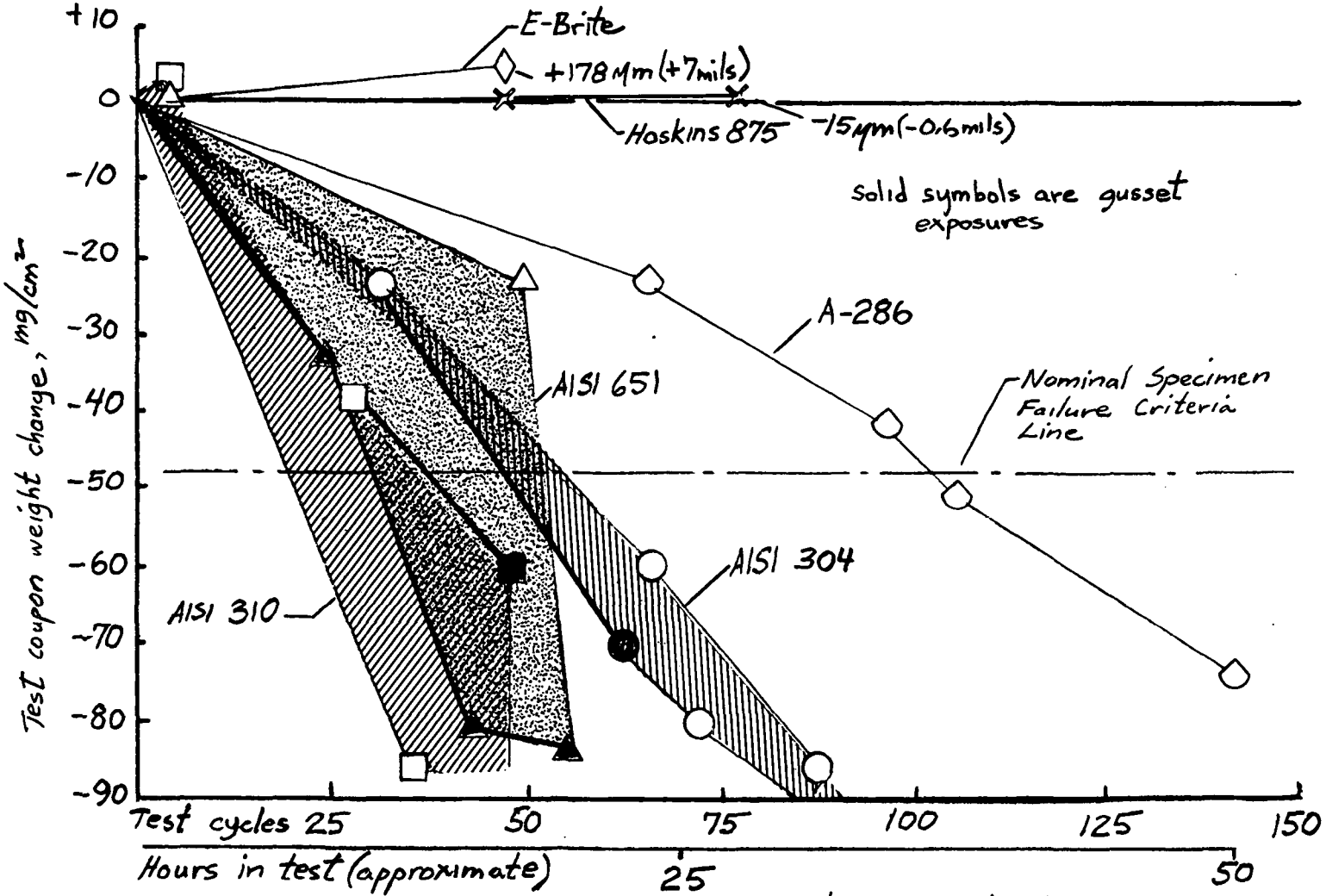

Figure 4.- Weight-change results for ferritic and austenitic iron alloy test coupons during cyclic screening test exposure at baffle and gusset locations in an automobile thermal reactor. Cycle consisted of 10 minute exposure at 1010°±30°C (1850°±50°F) followed by a 7 minute exposure with 510°C (950°F) minimum temperature.

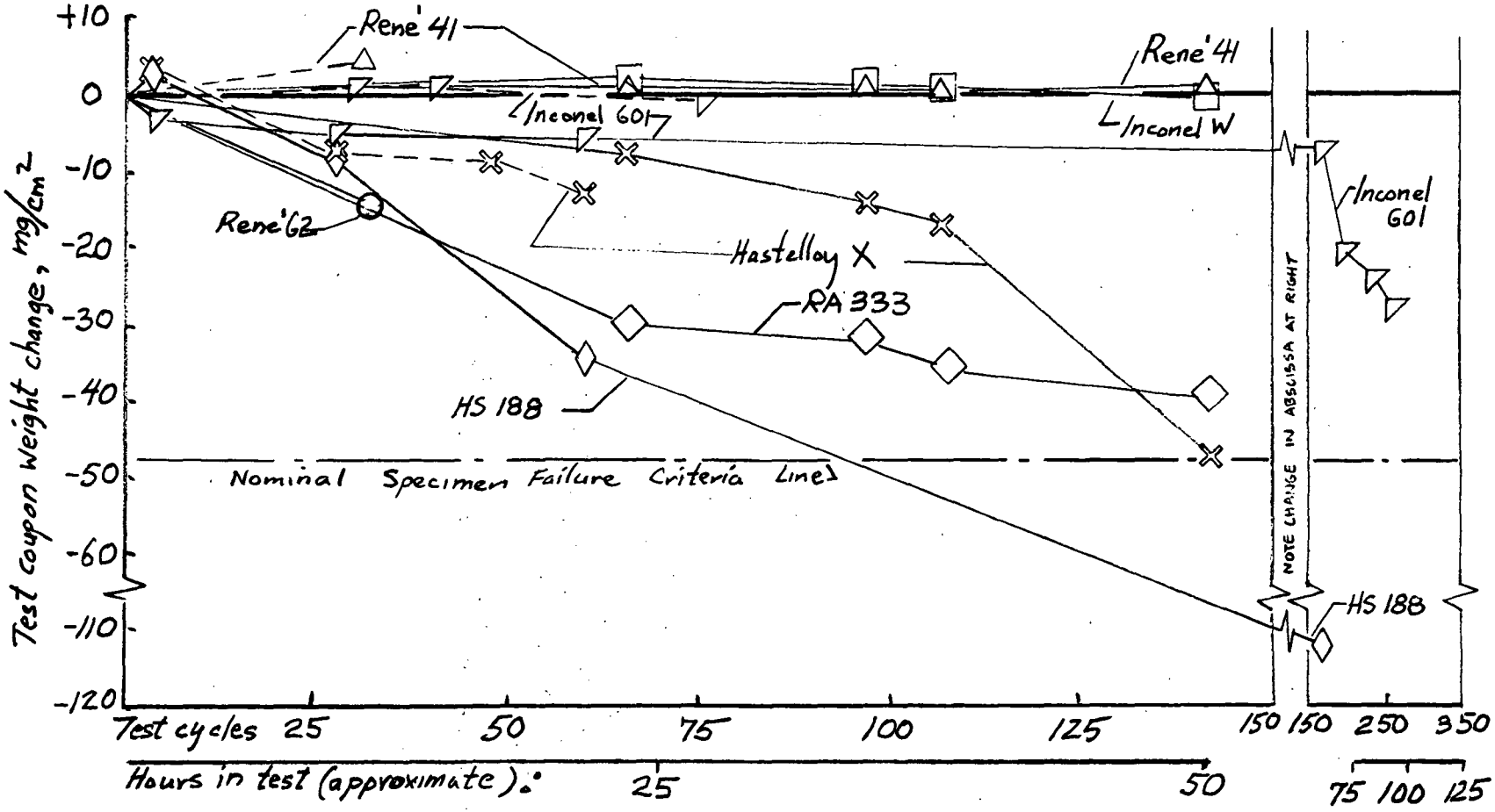

Figure 5.- Weight-change results for superalloy test coupons obtained during cyclic screening test exposure in an automobile thermal reactor. Cycle consisted of 10 minute exposure at 1010°±30°C (1850°±50°F) followed by a 7 minute exposure with 510°C (950°F) minimum test coupon metal temperature.

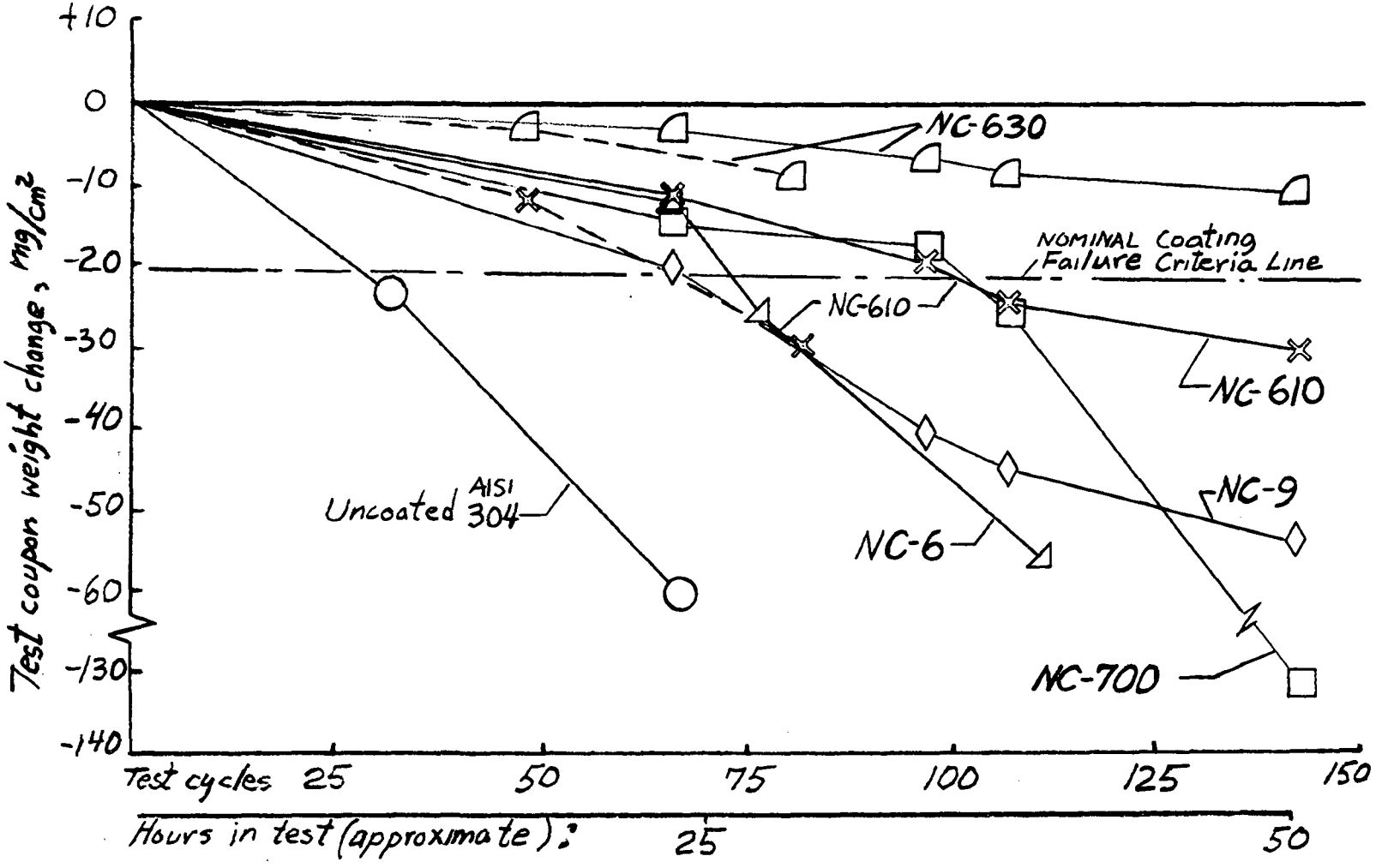

Figure 6.- Weight-change results for Ni-Cr coated AISI 304 test coupons during cyclic screening test exposure in an automobile thermal reactor. Cycle consisted of 10 minutes exposure at 1010°±30°C (1850°±50°F) followed by a 7 minute exposure with 510°C (950°F) minimum test coupon metal temperature.

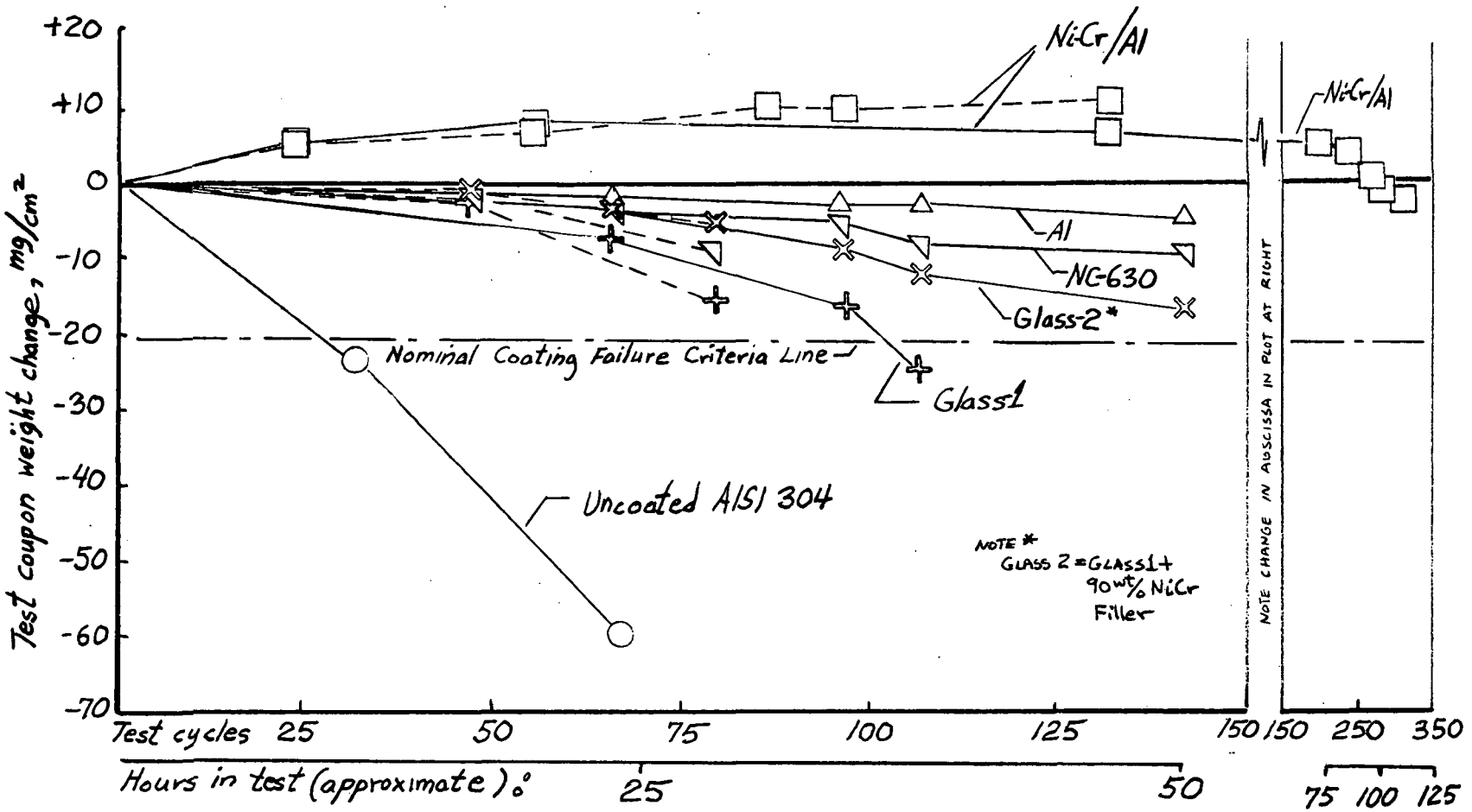

Figure 7.- Weight-change results for glass and aluminide-coated AISI 304 test coupons during cyclic screening test exposure in an automobile thermal reactor. Cycle consisted of 10 minute exposure at 1010° ± 30°C (1850° ± 50°F) followed by a 7 minute exposure with 510°C (950°F) minimum test coupon metal temperature.

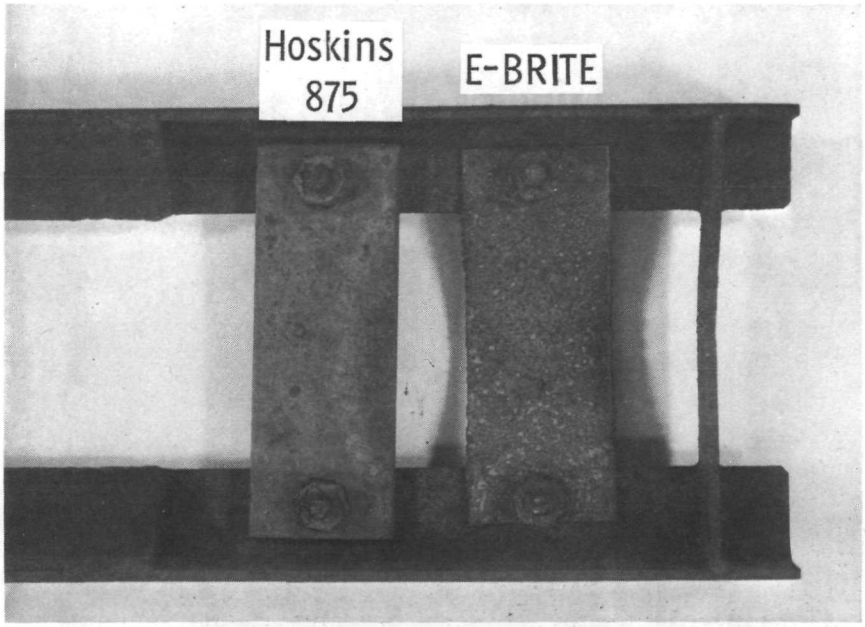

Figure 8. - Hoskins 875 and E-BRITE iron alloy test coupons after 48 test cycles (14.8 hours total exposure). X1.

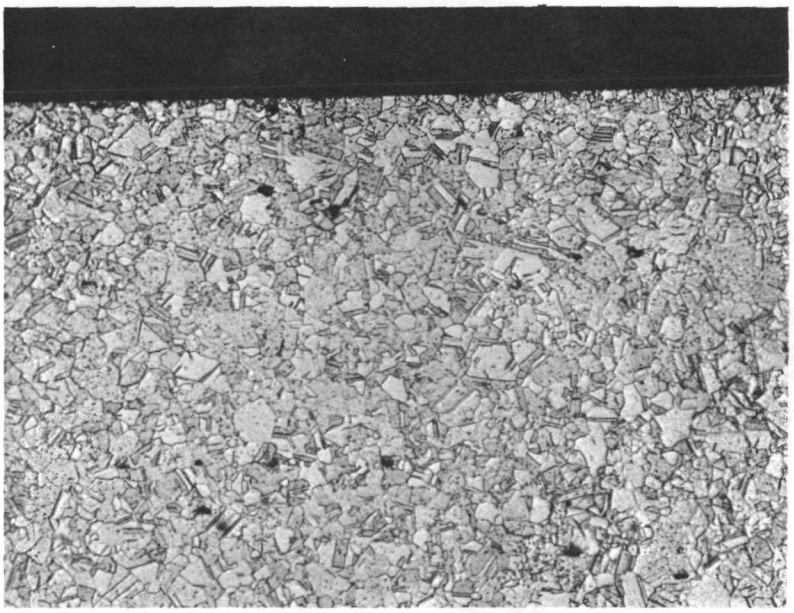

(a) As-received.

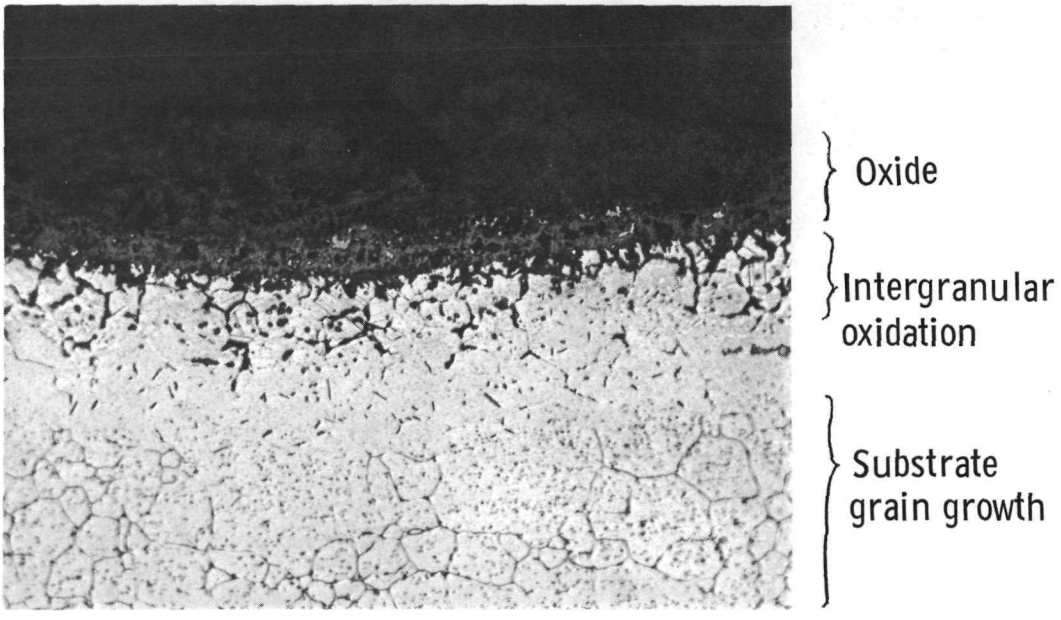

(b) After 267 test cycles.

Figure 9. - Uncoated Inconel 601 as-received and after 267 test cycles (136.1 hours total exposure). Etchant, $33H_2O$-$33HNO_3$-33 Acetic-1HF (by volume). X250.

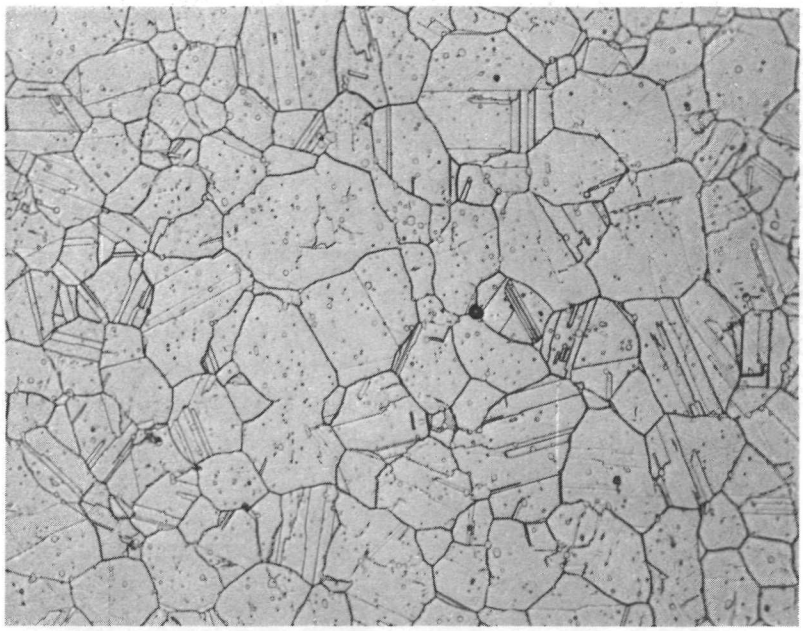

(a) As-received.

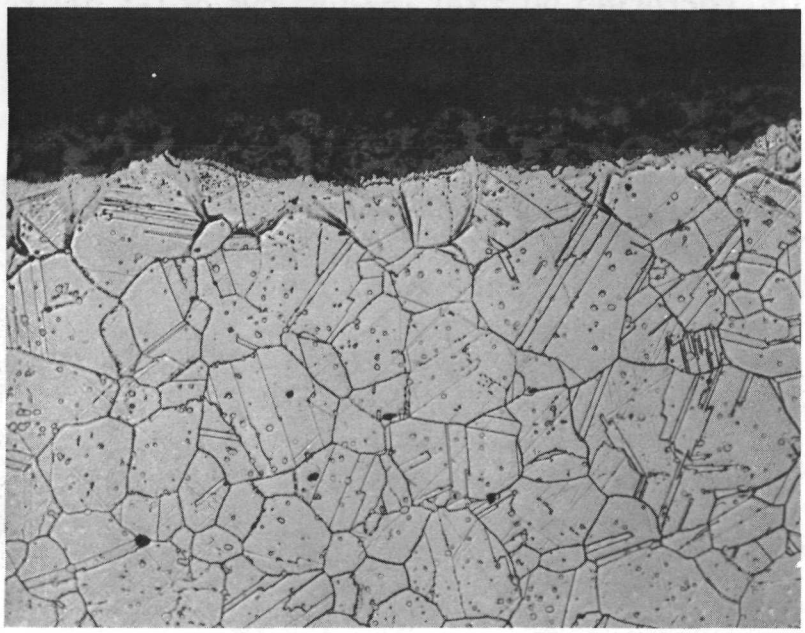

(b) After 170 test cycles.

Figure 10. - Uncoated HS-188 as-received and after 170 test cycles (100.9 hours total exposure). Etchant, HCl + peroxide (few drops), electrolytic. X250.

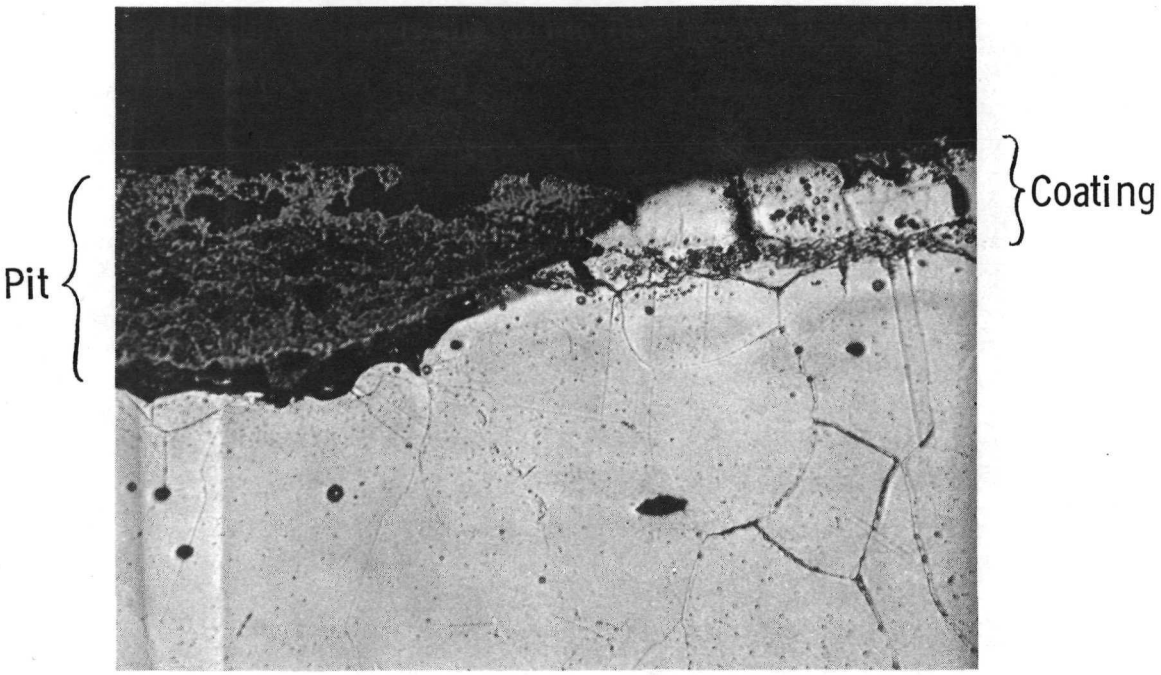

Figure 11. - Nickel-chromium coating NC-630 on AISI 304 showing corrosion pit after 142 test cycles (51 hours total exposure). Marble's Etchant; X250.

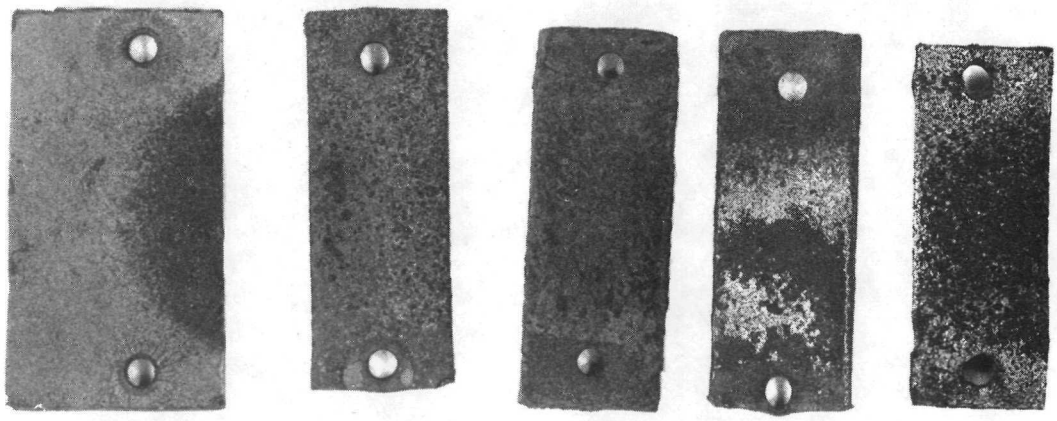

Al NC-630 NC-610 NC-9 Glass 2

Figure 12. - Aluminide and nickel-chromium coatings on AISI 304 test coupons after 142 test cycles (51 hours total exposure). X1.

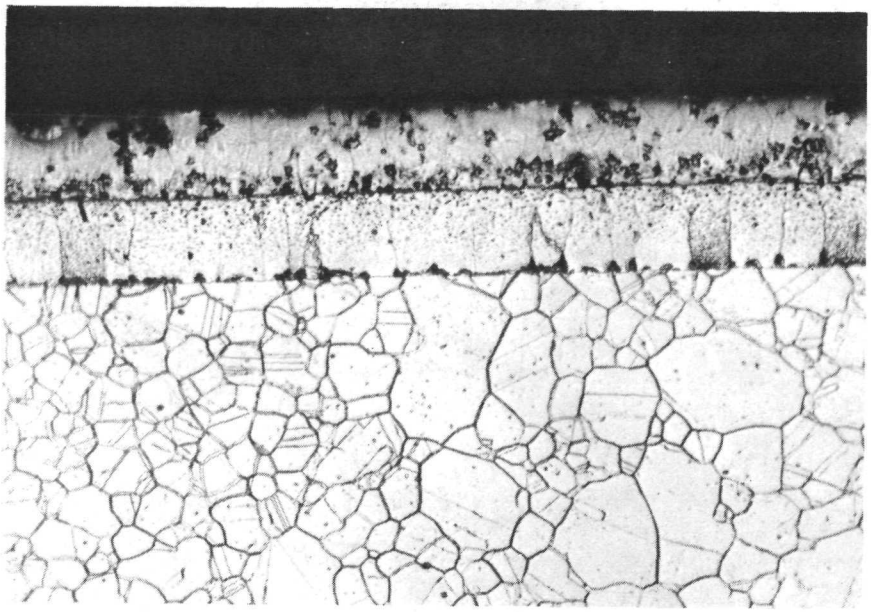

(a) As-received.

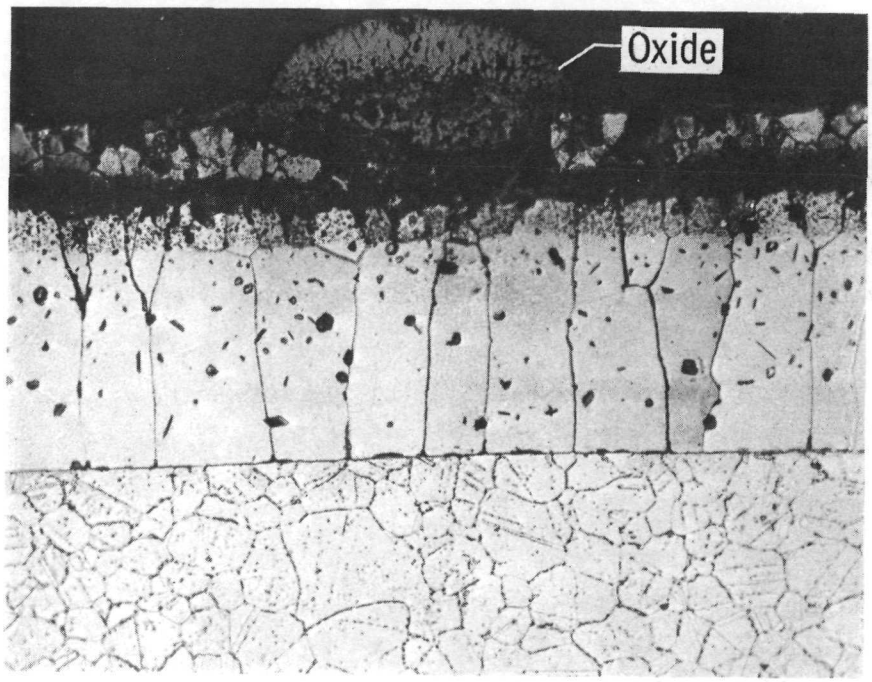

(b) After 142 test cycles.

Figure 13. - Aluminide (Al) coated AISI 304 as-received and after 142 test cycles (51 hours total exposure). Etchant, 75 ml glycerine and 25 ml aqua regia. X250.

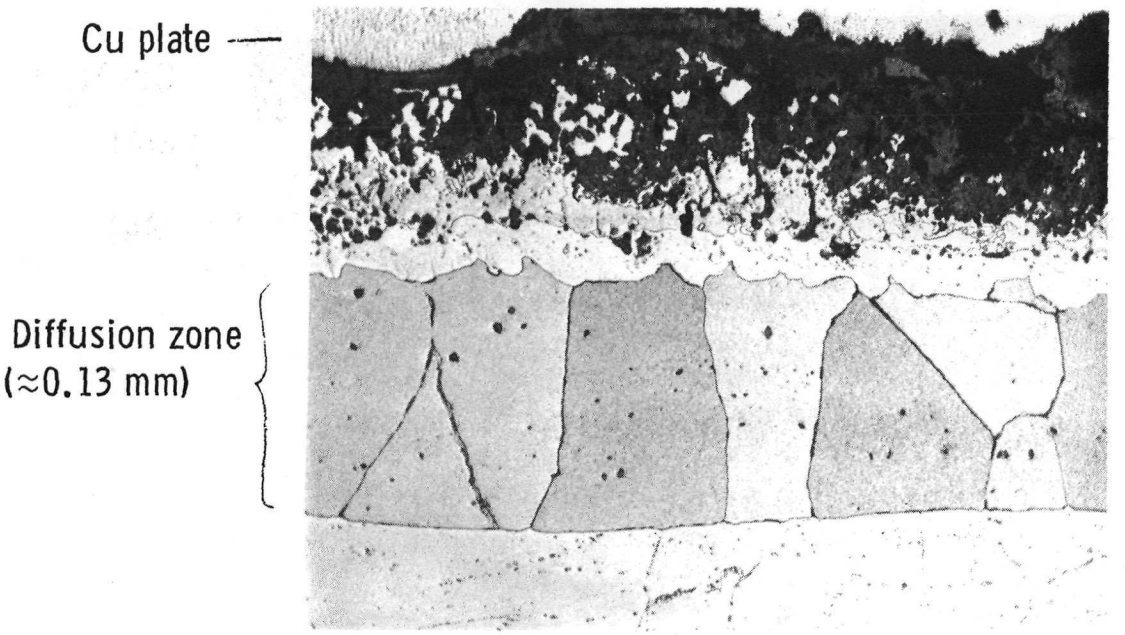

(a) After 132 test cycles.

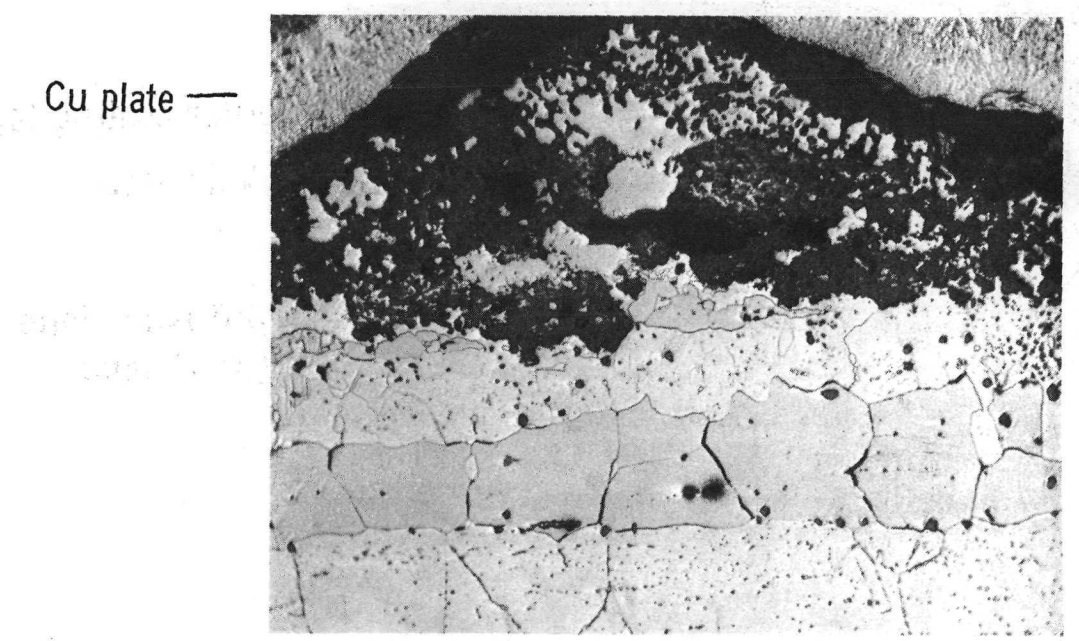

(b) After 308 test cycles.

Figure 14. - Aluminided nickel-chromium (Ni-Cr/Al) coated AISI 304 after 132 and 308 test cycles (47.8 and 108.9 hours total exposure, respectively). (The Cu-plate was applied in metallographic preparation.) Etchant, $33H_2O$-$33HNO_3$-33Acetic-$1HF_1$; X250.

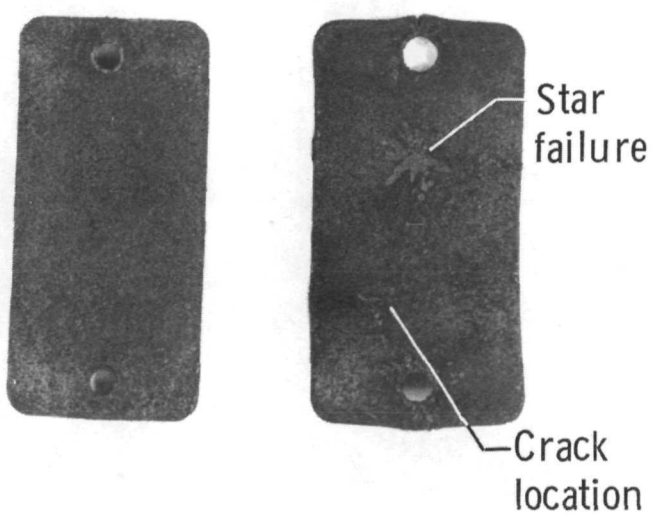

Test cycles: 132 308

Figure 15. - Aluminided nickel-chromium (Ni-Cr/Al) coated AISI 304 test coupons after 132 and 308 test cycles (47.8 and 108.9 hours total exposure, respectively). X1.